Hepatotoxicity Mediated by Pyrazole (CYP2E1) Plus TNF-α Treatment Occurs in *jnk2*−/− but not in *jnk1*−/− Mice

Xiaodong Wang, **Defeng Wu**, **Lili Yang**, and **Arthur I. Cederbaum**
Department of Pharmacology & Systems Therapeutics, Mount Sinai School of Medicine, New York, NY 10029, USA

Xiaodong Wang: xiaodong.wang@mssm.edu; Defeng Wu: defeng.wu@mssm.edu; Lili Yang: lili.yang@mssm.edu; Arthur I. Cederbaum: Arthur.cederbaum@mssm.edu

Abstract

CYP2E1 induction and TNF-α production are key risk factors in alcoholic liver injury. Increased oxidative stress from CYP2E1 induction by pyrazole in vivo sensitizes the liver to TNF-α-induced hepatotoxicity by a mechanism involving activation of c-jun N-terminal kinase (JNK) and mitochondrial damage. The goal of this study was to evaluate whether JNK1 or JNK2 plays a role in this potentiated hepatotoxicity. Wild type (wt), *jnk1*−/− and *jnk2*−/− mice were used to identify changes of hepatotoxicity, damage to mitochondria and production of oxidative stress following pyrazole plus TNF-α treatment. Increased serum ALT, inflammatory infiltration and central necrosis were observed in the *jnk2*−/− and wt mice treated with pyrazole plus TNF-α, but not in the *jnk1*−/− mice. Pyrazole elevated the activity and protein level of CYP2E1 in all mice. There was a significant increase of malondialdehyde, 4-hydroxynonenal adducts, 3-nitrotyrosine and inducible nitric oxide synthase in the *jnk2*−/− and wt mice compared to the *jnk1*−/− mice upon pyrazole plus TNF-α treatment, or compared to mice treated with either pyrazole alone or TNF-α alone. The antioxidants catalase, GPx-4, thioredoxin and glutathione were lowered and cytochrome c was released from the mitochondria in the *jnk2*−/− and wt mice. Mitochondrial production of superoxide was increased in the *jnk2*−/− and wt mice compared to the *jnk1*−/− mice upon pyrazole plus TNF-α treatment. Electron microscopy showed altered mitochondrial structure in the *jnk2*−/− and wt but not the *jnk1*−/− mice.

Conclusions—JNK1 plays a role in the hepatotoxicity, mitochondrial dysfunction and oxidative stress mediated by pyrazole plus TNF-α treatment. These findings raise the question as to the potential mechanisms of JNK1 activation related to alcoholic liver injury.

Keywords

Cytochrome P450 2e1; c-Jun N-terminal kinase; Oxidative stress; Liver injury; Mitochondrial damage

Introduction

Oxidative stress plays an important role in ethanol-induced liver injury (1–3). Many pathways play key roles in how ethanol induces oxidative stress, including impairment of mitochondrial function, enhanced production of TNF-α, and induction of CYP2E1 (4–6). In the intragastric model of chronic ethanol administration, liver injury coincided with an increase in TNF-α (7) and was prevented by anti-TNF-α antibody (5) and in mice lacking the TNFR1 receptor (8). These studies clearly implicate TNF-α as a major risk factor for the

Contact Information: Arthur I. Cederbaum, Ph.D., Department of Pharmacology and Systems Therapeutics, Mount Sinai School of Medicine, One Gustave L. Levy Place, New York, NY 10029. Tel: 212-241-7285; Fax: 212-996-7214; arthur.cederbaum@mssm.edu.

development of alcoholic liver injury. One complication in this central role for TNF-α is that hepatocytes are normally resistant to TNF-α induced toxicity. This led to the hypothesis that besides elevating TNF-α, alcohol somehow sensitizes or primes the liver to become susceptible to TNF-α (9). Results with hepatocytes, HepG2 E47 cells and Rala hepatocytes suggest that increased oxidative stress from CYP2E1 may sensitize isolated hepatocyes to TNF-α-induced toxicity (10,11).

Mice treated with pyrazole to elevate CYP2E1 were more susceptible to liver injury when treated with LPS or TNF-α compared to mice treated with pyrazole alone or LPS or TNF-α alone (12–14). Chlormethizole, an inhibitor of CYP2E1, blunted this elevated hepatotoxicity (12), and elevated toxicity was not found in CYP2E1 knockout mice (14). JNK or p38 MAPK play important roles in several models of liver injury, including CYP2E1-dependent toxicity (10,11,15–18). JNK MAP kinase was activated when mice were treated with pyrazole plus TNF-α but not when treated with pyrazole alone or TNF-α alone (14). The hepatotoxicity produced by pyrazole plus TNF-α was prevented by SP600125, an inhibitor of JNK (14). JNK is encoded for by 3 genes, each of which is alternatively spliced to yield α and β forms of both a 54 kDa and 46 kDa protein. In hepatocytes, only 2 of the genes, JNK1 and JNK2 are expressed (19). Mice deficient in either JNK1 or JNK2 are viable but double knockouts are embryonic lethal suggesting some redundant functions (19). JNK has been implicated in hepatic injury produced by TNF-α, ischemia-reperfusion, hepatitis virus, bile acids, alcohols and acetaminophen (15–18,20–22). In some models, JNK1 knockout mice did not develop liver injury, while in other models, mice depleted of JNK2 did not develop liver injury (17,18). The goal of the current study was to evaluate whether JNK1 or JNK2 or both play critical roles in the potentiation of TNF-α-induced hepatotoxicity and oxidative stress by pyrazole.

Materials and Methods

Experimental Models and Treatments

Animal experiments were performed with approval of the Mount Sinai Animal Care and Use Committee. Male $jnk1^{-/-}$ (B6.129-$Mapk8^{tm1Flv}$/J), $jnk2^{-/-}$ (B6.129-$Mapk9^{tm1Flv}$/J), and wild type, C57BL/6J mice (JNK1 KO, JNK2 KO and WT), weighing 24–26 g, at 8–10 weeks of age, were purchased from Jackson Laboratory (Bar Harbor, ME). JNK1 KO mice were backcrossed 7 generations to C57BL/6J mice while JNK2 KO mice were backcrossed 5 generations to C57BL/6J mice. Mice were divided into three groups and each strain received either pyrazole alone, TNF-α alone, or TNF-α following pyrazole pretreatment (Pyr/TNF group, n=4). Mice were injected intraperitoneally with pyrazole (Alfa Aesar, Ward Hill, MA), 150 mg/kg body weight, once a day for 3 days. Three hours after the second dose of pyrazole, the mice were administered TNF-α intraperitoneally (Fitzgerald, Acton, MA), 50 μg/kg body weight (pyrazole plus TNF-α group) or saline (pyrazole alone group). Other mice were treated with TNF-α, 50 μg/kg body weight (TNF-α alone group). At 24 hours after administration of TNF-α, the mice were sacrificed. Since neither treatment with pyrazole alone, nor TNF-α alone, at these concentrations, induced liver injury and produced results similar to saline-treated mice, the TNF-α alone or pyrazole alone groups were used as the none-injury mice to be compared to the TNF-α plus pyrazole-treated mice (see results).

Sample Collection, Pathology Analysis, and Biochemical Assays

Liver tissue collection and serum ALT was assayed as previously described (12–14). Morphological changes of liver tissues were observed by two pathologists who were blinded from the experimental information. Changes of degeneration and necrosis were graded as none (0), mild (<25%), moderate (25%–50%), and severe (>75%). Immunohistochemical

evaluation was marked as negative (−), weakly positive (+), moderately positive (++), and strongly positive (+++). Activities of CYP2E1, catalase, caspase 3 and 8, levels of MDA and GSH and TUNEL were assayed as previously described (12–14). Levels of ATP were assayed in liver homogenates using an ATP determination kit with recombinant firefly luciferase (Molecular Probes, Eugene, OR). Hepatic levels of TNF-α were assayed by ELISA. JNK activity was assayed in liver homogenates using a JNK in vitro kinase activity kit (Cell Signaling, Danvers, MA). Levels of the phosphorylated c-Jun fusion protein were detected after western blotting using a phospho-c-Jun antibody (17). Mitochondrial superoxide production *in situ* was determined as described by Minamiyama et al (23) using the oxidation-dependent fluorgenic dye, MitoSOX Red (5 μM) (Molecular probes, Carlsbad, CA).

Western Blot Analysis

Levels of CYP2E1, cytochrome c, Akt, TNFR1, mitochondrial thioredoxin (Trx-2), phospholipid hydroperoxide glutathione peroxidase (GPx-4), catalase, Cu-Zn superoxide dismutase-1, manganese superoxide dismutase-2 (SOD-1, SOD-2) and cox-4 in 20–100 μg of protein samples from freshly prepared microsome, cytosol, mitochondria, or homogenate fractions were determined using western blot analysis. Blots were scanned using Odyssey Imaging System (LI-COR Biosciences, Lincoln, NE). All specific bands were quantified with the Automated Digitizing System (ImageJ gel programs, version 1.34S, National Institute of Health).

Statistical Analysis—Values reflect means±SD. One-way ANOVA with subsequent post-hoc comparisons by Tukey HSD were performed by SPSS analysis software (version 10.0). *P* values of less than 0.05 were considered statistically significant and results are from experiments using 4 mice of each genotype.

Results

Serum Transaminases and Liver Morphological Changes

Severe pathological changes were detected in the WT mice treated with pyrazole plus TNF-α (Fig.1A3). but not in WT mice treated with pyrazole alone or TNF-α alone (Fig.1A1, A2). This liver injury was previously shown to be blunted by SP600125, a JNK inhibitor (14,24). Whether JNK1 or JNK2 or both play a role in this CYP2E1 plus TNF-α potentiated liver injury was evaluated by using JNK1 KO and JNK2 KO mice. Severe pathological changes, similar to those found in WT mice, were observed in JNK2 KO mice treated with pyrazole plus TNF-α (Fig.1A6), but not with pyrazole alone or TNF-α alone (Fig.1A4, A5). Many hepatocytes appeared to display significant ischemic necrosis and inflammatory infiltration in the hepatic centrilobular zone (Fig.1C) (Fig.1A). Some mild lesions were observed in the JNK1 KO group treated with pyrazole plus TNF-α, mainly dilation and congestion in the sinusoid, swelling and focal necrosis of hepatocytes in the centrilobular area. (Fig.1A9). Only mild degeneration of hepatocytes was found in JNK1 KO, JNK2 KO or WT mice after pyrazole alone or TNF-α alone administration. Serum ALT activities and the area of necrosis were significantly higher in the WT and JNK2 KO groups treated with pyrazole plus TNF-α than that in the JNK1 KO group treated with pyrazole plus TNF-α or in the WT and JNK2 KO groups treated with pyrazole alone or TNF- α alone (Fig.1B,1C). Levels of c-FLIP$_L$ and c-FLIP$_S$ (data not shown) and TNFR1 were similar for WT, JNK2 KO and JNK1 KO mice with all treatments (Fig.1E), and hepatic levels of TNF-α were also similar (Fig. 1D).

Caspase Activities and TUNEL Analysis

There was no significant difference in activity of either caspase 3 or casepase 8 in the 3 genotypes after the pyrazole plus TNF-α treatment (Fig.2A,2B). TUNEL results (Fig.2C,2D) showed that there were many hepatocytes with positive staining nuclei in the WT and JNK2 KO mice treated with pyrazole plus TNF-α compared to JNK1 KO group after pyrazole plus TNF-α treatment or in any group after pyrazole treatment alone or with TNF-α alone (Fig. 2C,2D). Positive staining was mainly in the centrilobular zone of the liver acinus.

CYP2E1 Protein and Activity

Western blot (Fig.3B) and immunohistochemistry showed that expression of CYP2E1 *in situ* was higher in all mice treated with pyrazole alone (Fig.3C1, C4, C7, ++-+++) compared to mice treated with TNF-α alone (Fig. 3C2, C5, C8, +). CYP2E1 catalytic activity was also higher in all pyrazole-treated mice (Fig.3A), confirming the elevation of CYP2E1 by pyrazole in all 3 groups. Similarly, expression of CYP2E1 was higher in all mice treated with pyrazole plus TNF-α (Fig.3C3, C6, C9, ++) compared to TNF-α alone. The positive expression of CYP2E1 was mainly in the centrilobular zone of the hepatic acinus, the area with the higher liver toxicity (Fig.1A,2D). CYP2E1 catalytic activity was also high in the JNK1 KO group after pyrazole plus TNF-α treatment (Fig.3A). CYP2E1 catalytic activity was however significantly lower in the WT and JNK2 KO mice treated with pyrazole plus TNF-α compared to the JNK1 KO mice treated with pyrazole plus TNF-α or the 3 groups treated only with pyrazole (Fig.3A). Thus, CYP2E1 activity, but not expression was lower in the WT and JNK2 KO mice which showed liver injury (elevated oxidative stress, see below).

Oxidative Stress, Lipid Peroxidation and iNOS Levels

4-HNE immunohistochemical staining and expression of 3-NT protein adducts were significantly stronger in the WT and JNK2 KO groups treated with pyrazole plus TNF-α (Fig.4C3, C6, +++;4E3, E6,++) compared to the JNK1 KO group treated with pyrazole plus TNF-α (Fig.4C9, +;4E9,+). There was only weak or negative 4-HNE staining or 3-NT protein adducts in all the groups treated with pyrazole alone or TNF- α alone (Fig.4C; 4E). The elevation of 4-HNE and 3-NT protein adducts in the WT and JNK2 KO mice were mainly found in the central lobular zone of the liver, the zone showing necrotic injury and elevated CYP2E1. There was an increase in iNOS in the central zone of WT and JNK2 KO groups after pyrazole plus TNF-α treatment (Fig.4D3, D6, ++-+++) compared to the JNK1 KO group treated with pyrazole plus TNF-α (Fig.4D9, +). There was only weak or negative staining in all groups treated with pyrazole alone or TNF-α alone (Fig.4D). MDA, an end product of LPO, was significantly higher while levels of GSH were significantly lower in homogenates of liver of the WT and JNK2 KO groups treated with pyrazole plus TNF-α compared to the JNK1 KO group treated with pyrazole plus TNF-α (Fig.4A;4B).

Antioxidants Changes

Catalase activity in liver homogenates was decreased in the WT and JNK2 KO groups treated with pyrazole plus TNF-α compared to the JNK1 KO group (Fig.5A). However, there was no significant difference of the catalase protein level in the 3 groups after pyrazole plus TNF-α treatment (Fig.5C). Levels of mitochondrial Trx-2 and homogenate GPx-4 protein were lower in the WT and JNK2 KO groups after pyrazole plus TNF-α treatment compared to the JNK1 KO group (Fig.5C). There was no effect on levels of cytosolic SOD-1 or mitochondrial SOD-2 protein in any group with any treatment (Fig.5C). TNF-α alone caused a modest activation of Akt in homogenates of all groups compared to pyrazole alone treated mice (Fig.5C). This small activation was lost in WT and JNK2 KO, but not JNK1 KO mice treated with pyrazole plus TNF-α (Fig.5C).

JNK activity was assayed via a JNK in-vitro kinase activity assay (17). In the JNK1 KO mice, treatment with pyrazole plus TNF-α (or TNF-α alone) produced a small increase in JNK kinase activity (Fig.5B). However, the pyrazole plus TNF-α treatment resulted in a decrease in JNK kinase activity in the WT and the JNK2 KO mice (Fig.5B). These results suggest that JNK kinase activity was elevated after pyrazole plus TNF-α treatment in the JNK1 KO, but not in the WT or JNK2 KO mice.

Mitochondrial Damage

The cytochrome c/cytochrome oxidase subunit 4 ratio decreased in the mitochondrial fractions of WT and JNK2 KO groups after pyrazole plus TNF-α treatment compared to JNK1 KO group or mice treated with pyrazole alone or TNF-α alone (Fig.6A). The cytochrome c/β-actin ratio increased in cytosolic fractions of the WT and JNK2 KO mice, but not in JNK1 KO mice after pyrazole plus TNF-α treatment (Fig.6A). Cox-4 was not detected in any cytosolic fraction. ATP levels were similar in the pyrazole alone treated groups (Fig.6B). Treatment with TNF-α alone produced a 30 to 40 % decline in ATP levels in all groups. Combined treatment with pyrazole plus TNF-α further lowerd ATP levels in all 3 groups (Fig.6B).

Levels of mitochondrial Trx-2 (Fig.5C) and mitochondrial GSH (Fig.6C) were lower in WT and JNK2 KO groups after pyrazole plus TNF-α treatment compared to the JNK1 KO group. Fluorescence of MitoSOX Red, a mitochondrial superoxide indicator, increased in livers from WT (Fig.6D3, +++) and JNK2 KO (Fig.6D6, +++) groups after pyrazole plus TNF-α treatment compared to the JNK1 KO (Fig.6D9, +) or compared to the mice treated with pyrazole alone or TNF-α alone. Electron microscopy observation showed mitochondrial swelling, broken cristae, and numerous lipid droplets in hepatocytes from the WT (Fig.6E1) and JNK2 KO (Fig.6E2) groups after pyrazole plus TNF-α treatment. Only mild mitochondrial swelling was observed in hepatocytes from the JNK1 KO (Fig.6E3) group treated with pyrazole plus TNF-α.

Discussion

Either LPS/TNF-α or CPY2E1 are considered independent risk factors involved in liver toxicity and alcoholic liver disease but mutual relationships or interactions between them have not been clearly defined. Increased oxidative stress from induction of CYP2E1 in vivo by pyrazole administration sensitizes hepatocytes to LPS and TNF-α toxicity and activation of JNK MAP kinase is a downstream mediator of this potentiated hepatotoxicity (12–14). Activation of the MAP kinase kinase kinase (ASK-1) was found in livers from mice treated with pyrazole plus TNF-α but not in livers from mice treated with pyrazole alone or TNF-α alone or in CYP2E1 knockout mice treated with pyrazole plus TNF-α (24). A model in which pyrazole plus TNF-α-elevated oxidative stress first activates ASK-1 via dissociation of the complex of thioredoxin, followed by ultimate activation of downstream MAP kinase kinase and then JNK was proposed as part of the injury mechanism. In these time course experiments, it was noted that JNK1 became activated prior to JNK2 (24). Whether this earlier and more pronounced activation of JNK1, relative to JNK2, plays a role in the elevation of hepatotoxicity and oxidative stress was the goal of this study.

JNK2 KO mice displayed hepatotoxicity similar to WT mice when treated with pyrazole plus TNF-α, however, JNK1 KO mice did not display this hepatotoxicity. No mice showed significant liver injury when treated with pyrazole alone or TNF-α alone. TUNEL positive staining was observed for the WT and JNK2 KO mice treated with pyrazole plus TNF-α but not the JNK1 KO mice. The elevated TUNEL staining may reflect necrotic but not caspase-dependent apoptotic DNA damage since activities of caspases 3 and 8 were similar for the three genotypes. The mitochondrial dysfunction in the pyrazole plus TNF-α-treated WT and

JNK2 KO mice may have caused a necrotic rather than an apoptotic mode of cell injury. Levels of ATP were lowest in all the pyrazole plus TNF-α treated mice which likely limits full blown apoptosis. Levels of CYP2E1 protein and activity were similar in the three genotypes treated with TNF-α alone. Induction of CYP2E1 protein and activity by pyrazole was found with all three genotypes. However, although CYP2E1 protein was increased, CYP2E1 catalytic activity was not elevated in the WT mice or JNK2 KO mice treated with pyrazole plus TNF-α. We speculate that this may be due to the hepatotoxicity and oxidative stress found with these two genotypes. Heme proteins such as cytochrome P450 are denatured by oxidants such as lipid hydroperoxides with a subsequent loss of catalytic activity (25). Thus, CYP2E1 catalytic activity but not CYP2E1 protein may not be elevated 24 hrs after addition of TNF-α to pyrazole-treated WT mice or JNK2 KO mice because of the hepatotoxicity and oxidative stress found with these mice but not in JNK1 KO mice at this time point. CYP2E1 catalytic activity is comparably elevated in pyrazole alone treated mice with all three genotypes, likely because there is no hepatotoxicity in these mice. In any event, the lack of hepatotoxicity (and elevated oxidative stress) in the pyrazole plus TNF-α-treated JNK1 KO mice is not due to failure to elevate CYP2E1 in these mice.

While ROS play an important role in activating JNK, increases in JNK can further elevate ROS (26,27). Several parameters associated with oxidative/nitrosative stress were elevated in the WT and the JNK2 KO mice, but not the JNK1 KO mice treated with pyrazole plus TNF-α. The increases in 4-HNE and 3-NT protein adducts and iNOS were largely in the pericentral zone of the liver acinus, the area where the liver injury was most pronounced. It is likely that the elevated oxidative/nitrosative stress is playing a central role in the hepatotoxicity found with the JNK2 KO mice, while the lack of an increase in oxidative/nitrosative stress in the JNK1 KO mice is preventive against hepatotoxicity. Oxidative stress may be enhanced because of decreases in survival factors such as pAkt or decreases in antioxidant protection e.g. GSH, Trx-2, GPx-4. Catalase activity was lowered in the WT and JNK2 KO mice compared to the JNK1 KO mice. The decline in catalase activity and levels of GSH, GPx-4 and Trx-2 would impact on effective removal of H_2O_2 in the WT and JNK2 KO mice. Note that catalase activity but not catalase protein was lowered in the WT and JNK2 KO mice (but not the JNK1 KO mice), results similar to the decline in CYP2E1 activity but not protein previously discussed. Catalase, like CYP2E1, is a heme enzyme; activity likely declines because of denaturation of the heme by the elevated oxidative stress as discussed for CYP2E1 catalytic activity.

JNK kinase activity was elevated in the JNK1 KO mice after treatment with pyrazole plus TNF-α, but decreased in the WT and the JNK2 KO mice. This may suggest that JNK2 signalling events after pyrazole plus TNF-α treatment are more pronounced upon depletion of JNK1. Loss of JNK2 caused increased activation of JNK1 in a mouse steatohepatitis model (17), and JNK2 interferred with JNK1 activation by TNF-α in fibroblasts (28). In general, JNK1, not JNK2, is believed to be most active in phosphorylation of c-Jun (17,28). Further studies are required to determine why JNK kinase activity is activated by pyrazole plus TNF-α in JNK1 KO mice and whether this plays a role in blunting the pyrazole plus TNF-α hepatotoxicity and oxidative stress in these mice. Recent studies have evaluated whether JNK1 or JNK2 play the more predominant role in potentiation of liver injury. In fibroblasts, JNK1 but not JNK2 appears to be essential for TNF-α-induced apoptosis (28). However, liver injury produced by either LPS/D-galactosamine or TNF-α/D-galacosamine was the same in WT and JNK1 KO mice but lower in JNK2 KO mice (29). JNK1 but not JNK2 promoted the development of steatohepatitis in mice fed a methionine choline-deficient diet (17). Singh et al (30) reported that JNK1 KO mice fed a high fat diet did not gain weight or develop steatohepatitis as did the WT and JNK2 KO mice. JNK2 was found to be predominant in acetaminophen toxicity (18). 6-hydroxydopamine-induced apoptosis in PC12 cells was JNK2 but not JNK1 dependent (31). While it has been suggested that JNK1

may promote cell death and JNK2 may promote proliferation and survival (21,28,32), it appears that depending on the toxin and cell type, either JNK1 or JNK2 or both play the major role in cell injury. Our results show that JNK1 plays the major role in the pyrazole plus TNF-α-induced liver injury, elevated oxidative stress and mitochondrial dysfunction.

It is not clear what activity JNK1 may catalyze that is not being catalyzed by JNK2, or vice versa, to explain the predominant role of JNK1 or JNK2 in promoting hepatotoxicity of a particular toxin or condition. Failure to activate caspase-8 or -3 or -7 was suggested as a possible reason why LPS/D-galactosamine was not toxic in the JNK2 KO mice (29), however, JNK1 appeared to be important for this activation in a steatohepatitis model (30). Activities of caspase-3 and -8 were comparable in the WT, JNK1 KO and JNK2 KO mice treated with pyrazole plus TNF-α. Toxicity in the WT and JNK2 KO mice was largely necrotic, not apoptotic as TUNEL staining did not correlate with caspase activities. We did not find significant differences in the levels of Bcl-2, Bcl-XL, Bax and Bak in livers of the three genotypes treated with pyrazole plus TNF-α (data not shown). Elevation of CYP2E1 protein levels was the same by pyrazole or pyrazole plus TNF-α in the three genotypes. There were no differences in TNF-α levels or levels of TNFR1 between the three genotypes to explain why JNK1 KO mice were protected against the pyrazole plus TNF-α toxicity whereas JNK2 KO mice were not. Levels of endoplasmic reticulum stress markers were not significantly elevated by pyrazole plus TNF-α treatment in all three genotypes (data not shown). In prostate cancer cells, it was concluded that TNF-α-induced ROS formation was mediated by JNK1 but not JNK2 and a mechanism involving ferritin degradation and increase in cellular non-heme iron pools was suggested (33). Hepatic iron levels were not determined in our study, nor whether iron chelators mitigate the pyrazole plus TNF-α toxicity and oxidative stress Proteomic and molecular modeling experiments may be helpful in identifying JNK1 target(s). Use of a liver specific JNK1 KO mouse model may also be helpful in determining whether differences between JNK1 and JNK2 in promoting the pyrazole plus TNF-α hepatotoxicity is specific to JNK actions in the liver, and not extrahepatic JNK actions. While elevated oxidative/nitrosative stress, decline in antioxidant protection, and mitochondrial dysfunction occur in the JNK2 but not JNK1 KO mice treated with pyrazole plus TNF-α, suggesting a role for JNK1 in interacting with and potentiating CYP2E1 toxicity, additional studies are necessary to identify specific target(s) for JNK1, but not JNK2, which play critical roles in the CYP2E1 plus TNF-α toxicity. Identifying JNK1 as the JNK isoform responsible for the liver injury, the elevated oxidative stress and the mitochondrial dysfunction, may have relevance in attempts to prevent or lower the hepatotoxicity by specifically inhibiting JNK1 without affecting JNK2.

Acknowledgments

List of Abbreviations

ALT	alanine aminotransferase
CYP2E1	cytochrome P450 2e1
GPx-4	phospholipid hydroperoxide glutathione peroxidase
GSH	reduced glutathione
HE	hematoxylin-eosin
4-HNE	4-hydroxynonenal

iNOS	inducible nitric oxide synthase
IHC	immunohistochemistry
JNK	c-Jun N-terminal kinase
KO	knock out
MAPK	mitogen activated protein kinase
MDA	malondialdehyde
3-NT	3-nitrotyrosine
PNP	p-nitrophenol
ROS	reactive oxygen species
TNF	tumor necrosis factor
TUNEL	terminal deoxynucleotidyl transferase-mediated dUTP nick-end labeling
WT	wild type

References

1. Albano E. Alcohol, oxidative stress and free radical damage. Proc Nutr Soc. 2006; 65:278–290. [PubMed: 16923312]

2. Bondy SC. Ethanol toxicity and oxidative stress. Toxicol Lett. 1992; 63:231–242. [PubMed: 1488774]

3. Nordman R, Riviere C, Rouach H. Implication of free radical mechanisms in ethanol-induced cellular injury. Free Rad Biol Med. 1992; 12:219–240. [PubMed: 1563648]

4. Bailey SM. A review of the role of reactive oxygen and nitrogen species in alcohol-induced mitochondrial dysfunction. Free Radic Res. 2003; 37:585–596. [PubMed: 12868485]

5. Iimuro Y, Gallucci RM, Luster MI, Kono H, Thurman RG. Antibodies to tumor necrosis factor alpha attenuate hepatic necrosis and inflammation caused by chronic exposure to ethanol in the rat. Hepatology. 1997; 26:1530–1537. [PubMed: 9397994]

6. Lieber CS. Cytochrome P4502E1: its physiological and pathological role. Physiol Rev. 1997; 77:517–544. [PubMed: 9114822]

7. Thurman RG. Mechanisms of hepatic toxicity. II. Alcoholic liver injury involves activation of Kupffer cells by endotoxin. Am J Physiol. 1998; 275:G605–G611. [PubMed: 9756487]

8. Yin M, Wheeler MD, Kono H, Bradford BU, Galluci RM, Luster MI, et al. Essential role of TNFα in alcohol-induced liver injury in mice. Gastroenterology. 1999; 117:942–952. [PubMed: 10500078]

9. Tsukamoto H. How is the liver primed or sensitized for alcoholic liver disease? Alcohol Clin Exp Res. 2001; 25:171S–181S. [PubMed: 11391068]

10. Pastorino JG, Hoek JB. Ethanol potentiates tumor necrosis factor-alpha cytotoxicity in hepatoma cells and primary rat hepatocytes by promoting induction of the mitochondrial permeability transition. Hepatology. 2000; 31:1141–1152. [PubMed: 10796891]

11. Liu H, Jones BE, Bradham C, Czaja MJ. Increased cytochrome P-450 2E1 expression sensitizes hepatocytes to c-Jun-mediated cell death from TNF-alpha. Am J Physiol Gastrointest Liver Physiol. 2002b; 282:G257–G266. [PubMed: 11804847]

12. Lu Y, Cederbaum AI. Enhancement by pyrazole of lipopolysaccharide-induced liver injury in mice: role of cytochrome P450 2E1 and 2A5. Hepatology. 2006; 44:263–274. [PubMed: 16799984]

13. Lu Y, Wang X, Cederbaum AI. Lipopolysaccharide-induced liver injury in rats treated with the CYP2E1 inducer pyrazole. Am J Physiol Gastrointest Liver Physiol. 2005; 289:G308–G319. [PubMed: 15845871]

14. Wu D, Cederbaum AI. Cytochrome P4502E1 sensitizes to tumor necrosis factor alpha-induced liver injury through activation of mitogen-activeted protein kineses in mice. Hepatology. 2008; 47:1005–1017. [PubMed: 18095305]

15. Liu H, Lo CR, Czaja MJ. NF-kappaB inhibition sensitizes hepatocytes to TNF-induced apoptosis through a sustained activation of JNK and c-Jun. Hepatology. 2002a; 35:772–778. [PubMed: 11915022]

16. Czaja MJ. The future of GI and liver research: editorial perspectives. III. JNK/AP-1 regulation of hepatocyte death. Am J Physiol Gastrointest Liver Physiol. 2003; 284:G875–G879. [PubMed: 12736142]

17. Schattenberg JM, Singh R, Wang Y, Lefkowitch JH, Rigoli RM, Scherer PE, et al. JNK1 but not JNK2 promotes the development of steatohepatitis in mice. Hepatology. 2006; 43:163–172. [PubMed: 16374858]

18. Gunawan BK, Liu ZX, Han D, Hanawa N, Gaarde WA, Kaplowitz N. c-Jun N-terminal kinase plays a major role in murine acetaminophen hepatotoxicity. Gastroenterology. 2006; 131:165–178. [PubMed: 16831600]

19. Davis RJ. Signal transduction by the JNK group of MAP kinases. Cell. 2000; 103:239–252. [PubMed: 11057897]

20. Schwabe RF, Uchinami H, Qian T, Bennett BL, Lemasters JJ, Brenner DA. Differential requirement for c-Jun NH2-terminal kinase in TNFα- and Fas mediated apoptosis in hepatocytes. FASEB J. 2004; 18:720–722. [PubMed: 14766793]

21. Qiao L, Han SI, Fang Y, Park JS, Gupta S, Gilfor D, et al. Bile acid regulation of C/EBPβ, CREB and c-Jun function via the extracellular signal-regulated kinase and c-Jun NH2 terminal kinase pathways, modulates the apoptotic response of hepatocytes. Mol Cell Biol. 2003; 23:3052–3066. [PubMed: 12697808]

22. Lee YJ, Shukla SD. Pro- and anti- apoptotic roles of c-Jun N terminal kinase (JNK) in ethanol and acetaldehyde exposed rat hepatocytes. Eur J Pharmacol. 2005; 508:31–45. [PubMed: 15680252]

23. Minamiyama Y, Takemura S, Toyokuni S, Imaoka S, Funae Y, Hirohashi K, et al. CYP3A induction aggravates endotoxemic liver injury via reactive oxygen species in male rats. Free Rad Biol Med. 2004; 37:703–712. [PubMed: 15288127]

24. Wu D, Cederbaum AI. Activation of ASK-1 and downstream MAP kinases in cytochrome P4502e1 potetiated TNFα liver injury. Free Rad Biol Med. 2010; 49:348–360. [PubMed: 20438834]

25. Lindstrom TD, Aust SD. Studies on cytochrome P450- dependent lipid hydroperoxide reduction. Arch Biochem Biophys. 1984; 233:80–87. [PubMed: 6431911]

26. Shen HM, Pervaiz S. TNF receptor superfamily-induced cell death: redox-dependent execution. FASEB J. 2006; 20:1589–1598. [PubMed: 16873882]

27. Schwabe RF, Brenner DA. Mechanisms of liver injury. TNFα-induced liver injury: role of IKK, JNK and ROS pathways. Am J Physiol GI Liver Physiol. 2006; 290:G583–G589.

28. Liu J, Minemoto Y, Lin A. C-Jun N-terminal kinase1 (JNK1) but not JNK2 is essential for TNFα-induced c-Jun kinase activation and apoptosis. Mol Cell Biol. 2004; 24:10844–10856. [PubMed: 15572687]

29. Wang Y, Singh R, Lefkowitch JH, Rigoli RM, Scherer PE, Czaja MJ. Tumor necrosis factor induced liver injury results from JNK2-dependent activation of caspase-8 and the mitochondrial death pathway. J Biol Chem. 2006; 281:15258–15267. [PubMed: 16571730]

30. Singh R, Wang Y, Xiang Y, Tanaka KE, Gaarde WA, Czaja MJ. Differential effects of JNK1 and JNK2 inhibition on murine steatohepatitis and insulin resistance. Hepatology. 2009; 49:87–96. [PubMed: 19053047]

31. Eminel S, Klettner K, Roemer L, Herdegan T, Waetzig V. JNK2 translocates to the mitochondria and mediates cytochrome relaease in PC12 cells in response to 6-hydroxydopamine. J Biol Chem. 2004; 279:55385–55392. [PubMed: 15504737]

32. Sabapathy K, Hochedlinger K, Nam SY, Bauer A, Karin M, Wagner EF. Distinct roles for JNK1 and JNK2 in regulating JNK activity and c-Jun- dependent cell proliferation. Mol Cell. 2004; 15:713–725. [PubMed: 15350216]

33. Antosiewicz J, Ziolkowski W, Kaczor JJ, Herman-Antosiewicz A. TNFα-induced reactive oxygen species formation is mediated by JNK1-dependent ferritin degradation and elevation of labile iron pool. Free Rad Biol Med. 2007; 43:265–270. [PubMed: 17603935]
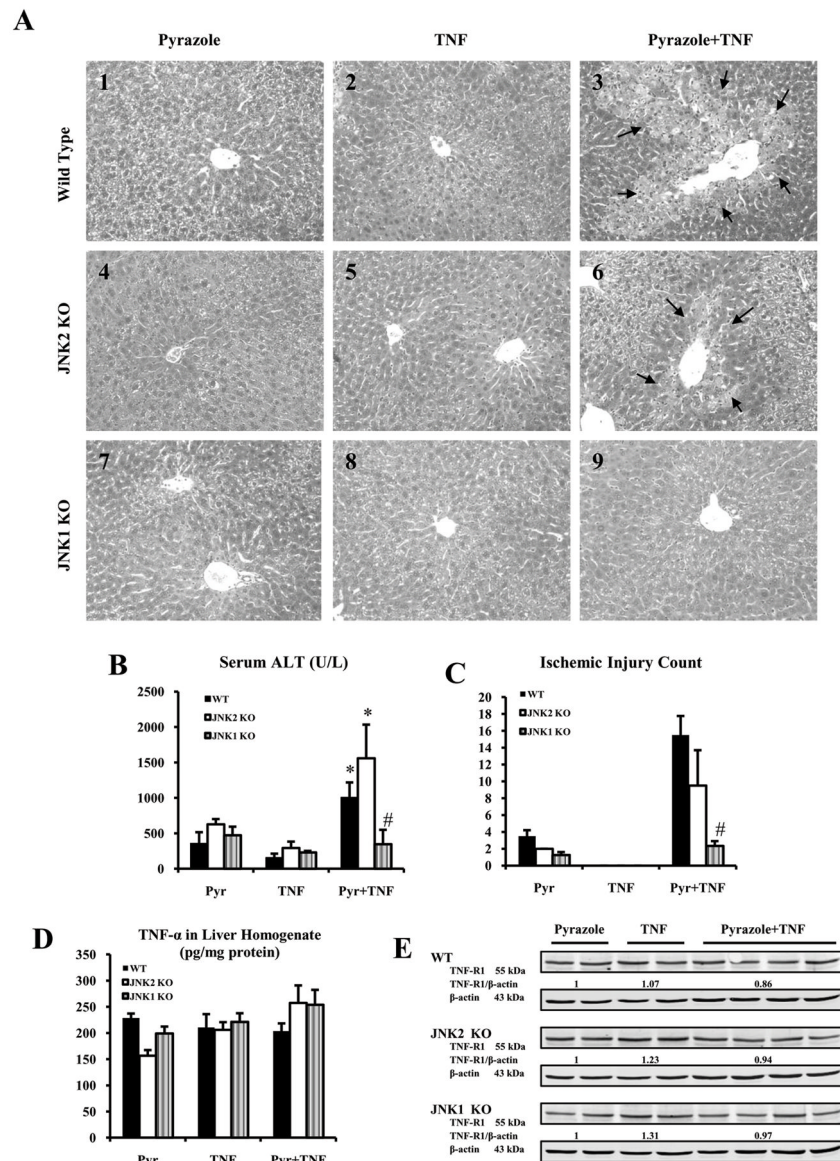
Fig.1.
Serum ALT, liver morphology and levels of TNF-α and TNFR1. (A) Histopathology. A3 and A6 show ischemic necrosis and infiltration of inflammatory cells in the central zone of the hepatic lobule (arrows, HE×300). A9 shows mild changes including hepatocyte swelling, vacuolating degeneration in the hepatic lobule. A1, A4 and A7 show mild changes including vacuolating degeneration and sinusoid congestion in the hepatic lobule. A2, A5, A8 shows no obvious pathological changes. (B) Serum ALT. (C) Ischemic injury count. (D) TNF-α in liver homogenate. (E) TNFR1 protein level. $p < 0.05$ compared to pyrazole alone or TNF-α alone,. # $p < 0.05$ compared to WT and JNK2 KO groups treated with pyrazole plus TNF-α.
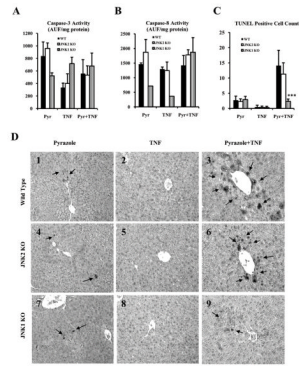
Fig.2.
Caspase-8 and caspase-3 activities and TUNEL staining. (A) Caspase-3 activity. (B) Caspase-8 activity. Results are expressed as arbitrary units of fluorescence per milligram of protein. (C) The number of apoptotic cells per high-powered field (HPF) as determined by TUNEL assay. (D) Apoptosis was assessed via TUNEL assay using the ApopTag in situ apoptosis detection kit. Positive apoptotic cells are indicated by arrows (TUNEL×300). *** $p < 0.001$ compared to WT and JNK2 KO groups treated with pyrazole plus TNF-α.
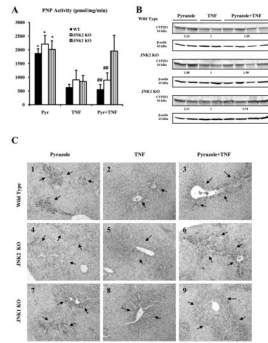
Fig.3.
CYP2E1 activity and protein levels. (A) CYP2E1 activity was measured by evaluating the oxidation of p-nitrophenol to p-nitrocatechol. *$p<0.05$ compared to groups treated with TNF-α,. ## $p<0.01$ compared to the JNK1 KO group treated with pyrazole plus TNF-α.. (B) CYP2E1 protein level. Numbers below the blots refer to the CYP2E1/β-actin ratio. (C) Immunohistochemical staining for CYP2E1. Slides were visualized with 3-amino-9-ethylcarbazole and positive staining was reflected by the red color and localized in the cytoplasm of hepatocytes in the central or intermediate lobular zone (arrows, IHC×300). In each case, a negative control (non-immune serum) was used.
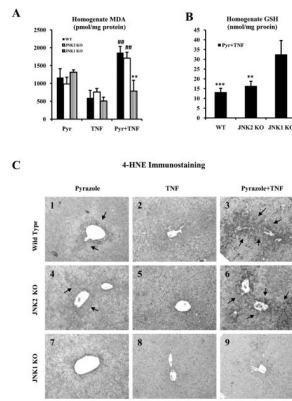
Fig.4.
Oxidative stress. (A) Thiobarbituric acid reactive substances (TBARS), expressed as malondialdehyde (MDA) equivalents. ** $p<0.01$ compared to the WT and JNK2 KO mice treated with pyrazole plus TNF-α. ## $p<0.01$ compared to pyrazole or TNF-α alone, (B) GSH in liver homogenates. ** $p<0.01$ and *** $p<0.001$ compared to the JNK1 KO treated with pyrazole plus TNF-α. (C) 4-HNE adducts. C3 and C6 show strong 4-HNE positive staining in hepatocytes from the pyrazole plus TNF-α treated WT mice and JNK2 KO mice (+++, arrows, IHC×300). C9 show weak 4-HNE positive staining in the JNK1 KO group (+, IHC×300). (D) iNOS. D3 and D6 (++-+++, arrows). D9 (+). (E) 3-NT adducts. E3 and E6 show moderate to strong 3-NT positive staining in hepatocytes from the WT and JNK2 KO mice (++-+++, arrows). E9 shows weak 3-NT positive staining in the JNK1 KO group (+).
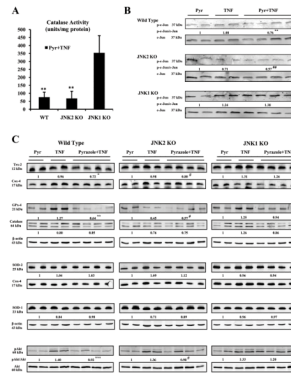
Fig.5.
Antioxidant levels and JNK kinase activity. (A) Catalase activity. ** *p*<0.05 compared to
JNK1 KO. (B) JNK kinase activity. Levels of the phosphorylated c-Jun fusion protein were
detected after western blotting using a phospho-c-Jun antibody. ** *p*<0.05 and ## *p*<0.05
compared to the pyrazole plus TNF-α-treated JNK1 KO mice. (C) Levels of Trx-2,
PHGPx-4, Catalase, pAkt/Akt, SOD-1 or SOD-2 protein in 20–100 μg of protein samples
from freshly prepared cytosol, mitochondria, or homogenate fractions were determined by
Western blot analysis using the Odyssey Imaging System. All specific bands were quantified
with the Automated Digitizing System.β-actin and cox-4 were assayed by Western blot and
results expressed as the catalase or GPx-4 or SOD-1/actin ratio or Trx-2 or SOD-2/cox-4
ratio or pAkt/Akt ratio below the specific blots. * *p*<0.05, ** *p*<0.01, *** *p*<0.001 and #
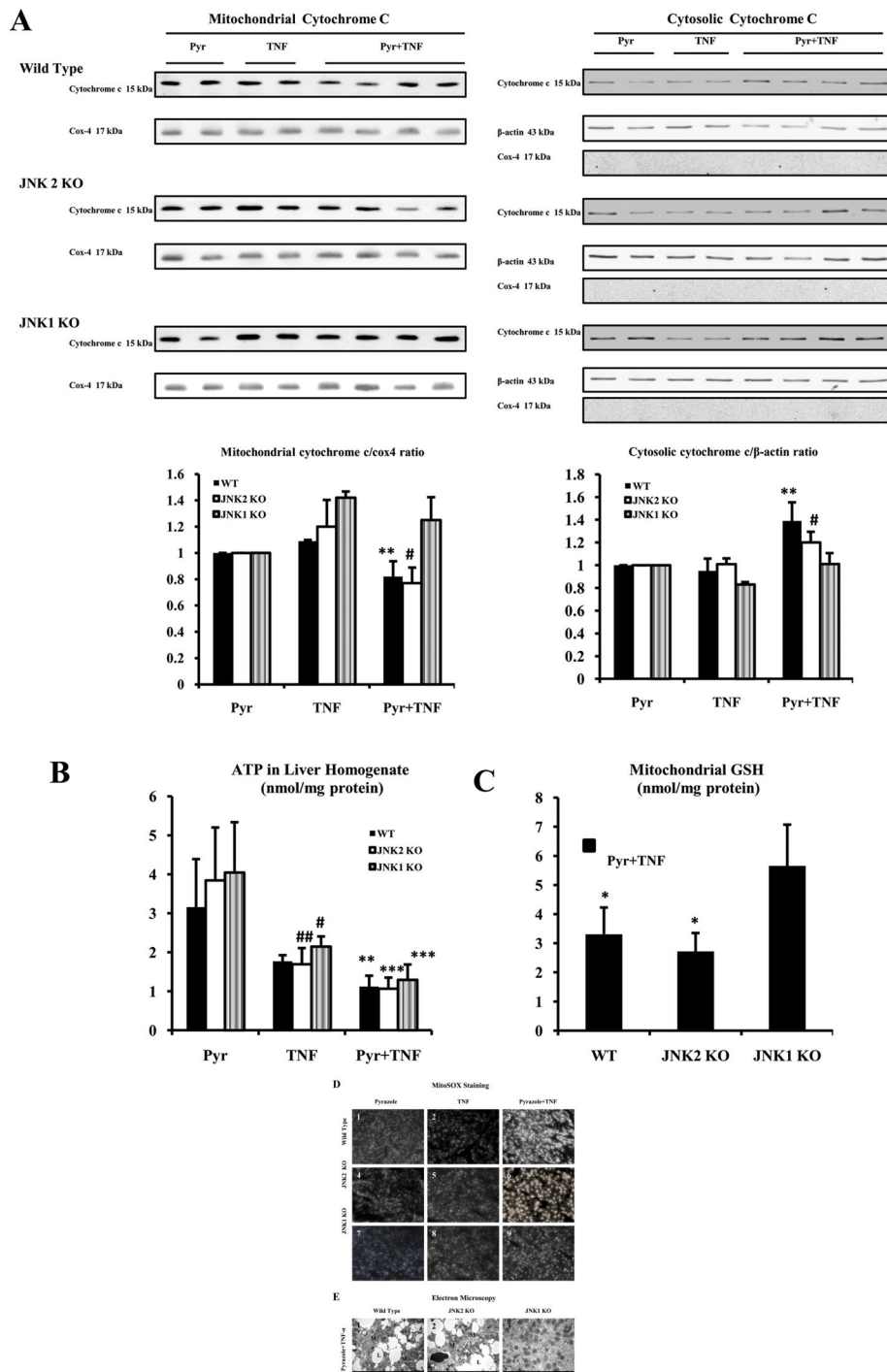*p*<0.05 compared to the pyrazole plus TNF-α-treated JNK1 KO mice.

Fig.6.
Mitochondrial assays. (A) Levels of cytochrome c protein in 20 μg of protein samples from freshly prepared cytosol and mitochondrial fractions. Cox-4 or β-actin was assayed by Western blot and results were expressed as the mitochondrial cytochrome c/cox-4 ratio or the cytosolic cytochrome c/actin ratio, # *p*<0.05 and ** *p*<0.01 compared to the pyrazole plus TNF-α-treated JNK1 KO mice. (B) ATP levels in liver homogenates were determined with recombinant firefly luciferase. ** *p*<0.01, *** *p*<0.001, # *p*<0.05 and ## *p*<0.01

compared to the pyrazole alone treatment. (C) Mitochondrial GSH. * $p<0.05$ compared to the JNK1 KO. (D) Fluorescence of the oxidation-dependent dye, MitoSOX Red. D3 and D6 show strong mitoSOX positive staining in hepatocytes from the WT and JNK2 KO mice treated with pyrazole plus TNF-α (+++, ×300). D9 shows weak mitoSOX positive staining in the JNK1 KO group treated with pyrazole plus TNF-α (+,×300). D1, D4 and D7(+); D2, D5 and D8 (+ or -). (E) Small liver fragments were immediately fixed in ice-cold 2% glutaraldehyde in phosphate-buffered saline and observed by transmission electron microscopy (M:mitochondria; L:lipid droplet). E1 shows severe damage of hepatocytes including lipid droplets and broken mitochondria (TEM×5000). E2 shows severe damage of hepatocyte including lipid droplets and broken mitochondria (TEM×5000). E3 shows hepatocyte with slight swelling of mitochondria (TEM×5000).